Family of oscillatory electromagnetic pulses

John Lekner
School of Chemical and Physical Sciences, Victoria University of Wellington, PO Box 600, Wellington, New Zealand

(Received 24 July 2023; accepted 3 November 2023; published 1 December 2023)

We discuss the properties of electromagnetic transverse electric and transverse magnetic (TE and TM) pulses based on a family of oscillatory solutions of the wave equation. The energy and momentum densities of the TE and TM pulses are annular. These pulses are sufficiently localized to have finite norm, total energy, momentum, and angular momentum, which are evaluated analytically. All the solutions given are proved to be strictly forward propagating (unidirectional). The wave function is characterized by a length a and a wave number K. The longitudinal extent of the pulses and the number of oscillations are of order $2a$ and Ka, respectively. Far from the focal region, the annular TE and TM pulses diverge from the axis of propagation on a cone, the angle of which is determined.

DOI: 10.1103/PhysRevA.108.063502

I. INTRODUCTION

The wave equation goes back to d'Alembert and Euler (for the one- and three-dimensional cases, respectively). This paper is about solutions $\psi(\boldsymbol{r},t)$ of the wave equation sufficiently localized in space-time to have finite norm $N = \int d^3r\ |\psi(\boldsymbol{r},t)|^2$, and, for the electromagnetic pulses derived from $\psi(\boldsymbol{r},t)$, finite total energy and total momentum. We also insist that the pulses be unidirectional, by which we mean that no part of the pulse has negative momentum component in the direction of propagation. We prove that the transverse electric (TE) and transverse magnetic (TM) pulses formed from a general superposition of the product of plane longitudinal and Bessel-function transverse solutions of the wave equation are all strictly forward propagating.

Recent interest in optics is in very short pulses, with a small number of cycles. We shall give the properties of a class of solutions characterized by a length and a wave number: their norm, and the energy and momentum of the transverse electric and transverse magnetic pulses formed from them. The pulses can be subcycle to many cycle, depending on the (freely chosen) length and wave-number parameters.

We first give an example of existing solutions. So, Plachenov and Kiselev [1] discovered a simple unidirectional and localized solution of the wave equation, u_+. In cylindrical coordinates (ρ,ϕ,z), the simplest version of u_+ is (we normalize the wave function to unity at the space-time origin)

$$G(\rho,z,t) = \frac{a^2}{R(R-iz)},\ R^2 = (a+ict)^2+\rho^2. \tag{1.1}$$

The author [2] has found a *family* of solutions of the wave equation, of which the simplest form is

$$\Psi_0(\rho,z,t) = \frac{F(R-iz)}{R}$$
$$(F \text{ is any twice} - \text{differentiable function}). \tag{1.2}$$

An additional length parameter b may be introduced by a complex translation in z, $z \to z-ib$, as discussed in Ref. [3] (Sec. 2.6 and Appendix 2B). Solutions of the wave equation with azimuthal dependence of the form $e^{im\phi}$ may be obtained by operating repeatedly with $\partial_x + i\partial_y = e^{i\phi}(\partial_\rho + i\rho^{-1}\partial_\phi)$; for example, $\Psi_1(\rho,\phi,z,t) = e^{i\phi}\partial_\rho \frac{F(R-iz)}{R}$.

This paper is an exploration of the properties of oscillatory pulses formed by setting $F(X) = X^{-1}\exp(-KX)$, namely

$$G_K(\rho,z,t) = a^2\, e^{Ka}\, \frac{e^{iKz-KR}}{R(R-iz)}. \tag{1.3}$$

We note that $G_K \to G$ in the limit $K \to 0$.

In Sec. II we shall give the basic properties of such pulses, as functions of the length parameter a, and the wave number K, both assumed to be positive. Section III will examine the properties of TE and TM pulses formed from G_K, and give graphical examples. Section IV proves that for pulses based on a large class of solutions of the wave equation (which includes G_K) *there is no backflow*. This section also compares and contrasts the isophase surfaces of G_K pulses and of monochromatic beams. Section V gives estimates of the TE and TM pulse extent, and of the angle at which they converge onto or diverge from the axis of propagation.

II. PROPERTIES OF PULSES IN TERMS OF THEIR WAVE-NUMBER WEIGHT FUNCTION

Forward-propagating solutions of the wave equation may be put in the form (Ref. [3], Sec. 2.4)

$$\psi_m(\rho,\phi,z,t) = e^{im\phi}\int_0^\infty dk\, e^{-ikct}\int_0^k dq w(k,q) e^{iqz} J_m(\kappa\rho),$$
$$\kappa = \sqrt{k^2-q^2}. \tag{2.1}$$

Proof of the unidirectionality of TE and TM pulses based on (2.1) will be given in Sec. IV.

The wave-number weight function $w(k,q)$ determines the wave function ψ_m. For the function G_K the azimuthal quantum number m is zero, and the weight function is

$$w(k,q) = \begin{cases} a^2\, e^{(K-k)a}, & k \geqslant K,\ q \geqslant K \\ 0, & \text{otherwise} \end{cases}. \tag{2.2}$$

The factor $a^2\, e^{Ka}$ normalizes the wave function to unity at the space-time origin. The remaining exponential decay factor e^{-ka} provides the scale length a. Note the all-important cutoff: both the total wave number k and its longitudinal component q must exceed the characteristic wave number K.

The norm $\int d^3r\ |\psi_m|^2$, for a given wave function ψ_m defined by (2.1), is given by Ref. [3], Sec. 2.4 (we have changed the variable of integration from κ to q).

$$N = \int d^3r\ |\psi_m|^2 = (2\pi)^2 \int_0^\infty dk\, k^{-1} \int_0^k dq\ |w(k,q)|^2. \tag{2.3}$$

For the weight function given in (2.2) the norm evaluates to

$$N = 2\pi^2\, a^3\{1 - 2Kae^{2Ka}\mathrm{Ei}_1(2Ka)\},$$
$$\mathrm{Ei}_1(\alpha) = \int_1^\infty dy\, y^{-1} e^{-\alpha y}\ (\alpha > 0). \tag{2.4}$$

The wave-number weight function $w(k,q)$ also determines the total energy, total momentum, and total angular momentum of particular electromagnetic pulses based on the wave function (2.1). For both the transverse electric and the transverse magnetic pulses these are given by [4]

$$U = \int d^3r\ u(\boldsymbol{r},t)$$
$$= \frac{\pi}{2}\int_0^\infty dk \int_0^k dq |w(k,q)|^2\ (k^2 - q^2)k, \tag{2.5}$$
$$cP_z = c\int d^3r\ p_z(\boldsymbol{r},t)$$
$$= \frac{\pi}{2}\int_0^\infty dk \int_0^k dq |w(k,q)|^2 (k^2 - q^2)q, \tag{2.6}$$
$$cJ_z = c\int d^3r\rho\ p_\phi$$
$$= \frac{\pi}{2}\int_0^\infty dk \int_0^k dq |w(k,q)|^2 (k^2 - q^2)m. \tag{2.7}$$

The energy, momentum, and angular momentum densities are the same for the TE and TM pulses, as we shall see in the next section.

The expressions (2.5) to (2.7) for the total energy, momentum, and angular momentum show that a classical electromagnetic wave packet can be thought of as a superposition of light quanta, with energies $\hbar ck$, z components of momenta and of angular momenta $\hbar q$ and $\hbar m$.

For the $m = 0$ wave function (1.3), corresponding to the wave-number weight function (2.2), we find from (2.5) and (2.6) that

$$U = \frac{\pi}{16a}(4 + 5Ka + 2K^2 a^2),$$
$$cP_z = \frac{\pi}{32a}(3 + 6Ka + 4K^2 a^2). \tag{2.8}$$

(It is understood that these values, obtained from a dimensionless solution of the wave equation, are to be multiplied by a factor of dimension *energy* times *length*.) The expressions in (2.8) can be verified by integration over all space of the energy and momentum densities to be derived in in Sec. III. Note that $cP_z < U$ for all values of Ka, in accord with the general theorem (Ref. [5], Sec. 16.5 and Problem 16.17; Ref. [3], Sec. 1.4). Such pulses may be Lorentz transformed to a zero-momentum frame [6–10], and one may accordingly associate a mass with each pulse [11]. The behavior of the ratio cP_z/U at small and large Ka is

$$\frac{cP_z}{U} = \frac{3}{8} + \frac{9Ka}{32} + O(Ka)^2, \quad \frac{cP_z}{U} = 1 - \frac{1}{Ka} + O(Ka)^{-2}. \tag{2.9}$$

When $Ka \ll 1$, Eq. (2.8) gives the energy and momentum of pulses formed from G. In the large-Ka limit the TE and TM pulses based on G_K have the textbook ratio of momentum to energy, associated with electromagnetic plane waves.

III. ELECTROMAGNETIC TE AND TM PULSES BASED ON G_K

Free-space electromagnetic fields which satisfy the Maxwell equations may be constructed from a vector potential $\boldsymbol{A}(\boldsymbol{r},t)$ and a scalar potential $V(\boldsymbol{r},t)$ which satisfy the wave equation and the Lorenz condition $\nabla\cdot\boldsymbol{A} + \partial_{ct}V = 0$. For example, in Cartesian coordinates $[x, y, z]$, the choice $V =$ constant, $\boldsymbol{A} = \nabla\times[0,\ 0,\ \psi] = [\partial_y,\ -\partial_x,\ 0]\psi$ satisfies the Lorenz condition, and gives us the transverse electric (TE) pulse with

$$\boldsymbol{E} = -\partial_{ct}A = [-\partial_y\partial_{ct},\ \partial_x\partial_{ct},\ 0]\psi,$$
$$\boldsymbol{B} = \nabla\times\boldsymbol{A} = \left[\partial_x\partial_z,\ \partial_y\partial_z,\ -\partial_x^2 - \partial_y^2\right]\psi. \tag{3.1}$$

In cylindrical polars the complex fields simplify to

$$\boldsymbol{E} = (-im\rho^{-1}\partial_{ct},\ \partial_\rho\partial_{ct},\ 0)\psi,$$
$$\boldsymbol{B} = \left(\partial_\rho\partial_z,\ im\rho^{-1}\partial_z,\ \partial_z^2 - \partial_{ct}^2\right)\psi. \tag{3.2}$$

We have assumed azimuthal variation $e^{im\phi}$, as in Eq. (1.2), and that ψ satisfies the wave equation. Note that in the plane-wave limit, $\psi \to e^{iK(z-ct)}$, the fields vanish.

When $m = 0$ the TE pulse has one nonzero $\boldsymbol{E}$ component, the azimuthal one. Its electric field is therefore linearly polarized, but the direction of polarization is not fixed in space: the field lines are circles, centered on the propagation axis.

Both the real and the imaginary parts of ψ are solutions of the wave equation, giving two physical fields, the real and imaginary parts of (3.2):

$$\boldsymbol{E}_r = (m\rho^{-1}\partial_{ct}\psi_i,\ \partial_\rho\partial_{ct}\psi_r,\ 0),$$
$$\boldsymbol{B}_r = \left(\partial_\rho\partial_z\psi_r,\ -m\rho^{-1}\partial_z\psi_i,\ \partial_z^2\psi_r - \partial_{ct}^2\psi_r\right), \tag{3.3}$$

$$\boldsymbol{E}_i = (-m\rho^{-1}\partial_{ct}\psi_r,\ \partial_\rho\partial_{ct}\psi_i,\ 0),$$
$$\boldsymbol{B}_i = \left(\partial_\rho\partial_z\psi_i,\ m\rho^{-1}\partial_z\psi_r,\ \partial_z^2\psi_i - \partial_{ct}^2\psi_i\right). \tag{3.4}$$

A TM pulse is obtained from the TE pulse by the *duality transformation* $\boldsymbol{E}\to\boldsymbol{B}$, $\boldsymbol{B}\to-\boldsymbol{E}$. The duality transformation leaves the energy density $u = \frac{1}{8\pi}(E^2 + B^2)$ and the momentum density $\boldsymbol{p} = \frac{1}{4\pi c}\boldsymbol{E}\times\boldsymbol{B}$ unchanged. Thus, for both TE and TM pulses, with the fields given in (3.3) we have

$$8\pi u = (\partial_\rho\partial_z\psi_r)^2 + (\partial_\rho\partial_{ct}\psi_r)^2 + \left[\partial_z^2\psi_r - \partial_{ct}^2\psi_r\right]^2$$
$$+ m^2\rho^{-2}[(\partial_z\psi_i)^2 + (\partial_{ct}\psi_i)^2], \tag{3.5}$$

$$4\pi c p_\rho = E_\phi B_z - E_z B_\phi = E_\phi B_z = (\partial_\rho \partial_{ct}\psi_r)\big(\partial_z^2\psi_r - \partial_{ct}^2\psi_r\big), \tag{3.6}$$

$$4\pi c p_\phi = E_z B_\rho - E_\rho B_z = -E_\rho B_z = -m\rho^{-1}(\partial_{ct}\psi_i)\big(\partial_z^2\psi_r - \partial_{ct}^2\psi_r\big), \tag{3.7}$$

$$4\pi c p_z = E_\rho B_\phi - E_\phi B_\rho = -m^2\rho^{-2}(\partial_{ct}\psi_i)(\partial_z\psi_i) - (\partial_\rho\partial_{ct}\psi_r)(\partial_\rho\partial_z\psi_r). \tag{3.8}$$

The energy density u is non-negative. The ϕ component of the momentum density is proportional to the azimuthal winding number m, and hence so is the angular momentum density component along the direction of propagation, $j_z = xp_y - yp_x = \rho p_\phi$. For a TE or TM pulse formed from the real parts of the fields,

$$j_z = -\frac{m}{4\pi c}(\partial_{ct}\psi_i)\big(\partial_z^2\psi_r - \partial_{ct}^2\psi_r\big). \tag{3.9}$$

The energy- and momentum densities obtained by choosing the fields (3.4) have the same form, with ψ_r and ψ_i interchanged and a change of sign in p_ϕ (and hence of j_z).

Figures 1 and 2 show the energy and the momentum densities for the case $Ka = 2$. Figure 1 is based on the fields of (3.3), the real parts of (3.2); Fig. 2 is based on (3.4), the imaginary part of (3.2).

Figures 3 and 4 show the energy and the momentum densities for the case $Ka = 2\pi$. Figure 3 is based on the fields of (3.3), the real parts of (3.2); Fig. 4 is based on (3.4), the imaginary part of (3.2).

We see from Figs. 1–4 that the TE and TM pulses based on G_K are *annular,* with a complex structure in their focal region (here coinciding with the space-time origin), but becoming more simply organized as they diverge away from the focal region. The longitudinal component of the momentum density p_z is zero on the axis $\rho = 0$ when $m = 0$. This follows from (2.1) and (3.6): $\partial_\rho J_0(\kappa\rho) = -\kappa J_1(\kappa\rho)$, and this is zero when $\rho = 0$. When $m = 0$ the momentum-density component p_ρ is also zero on axis, for the same reason, and p_ϕ is identically zero.

IV. ABSENCE OF BACKFLOW IN TE AND TM PULSES

Backflow (regions where $p_z < 0$) follows from the topologically necessary zeros in the focal region of electromagnetic beams (Ref. [12], Sec. 1.6); it also arises in the superposition of plane electromagnetic waves [13].

Here we give a proof of the absence of backflow for TE and TM pulses based on the integral representation of the wave function,

$$\psi(\rho,z,t) = \int_0^\infty dk e^{-ikct}\int_0^k dq w(k,q)e^{iqz}J_0(\kappa\rho) = \frac{1}{2\pi}\int_{-\pi}^{\pi}d\chi\int_0^\infty dk e^{-ikct}\int_0^k dq w(k,q) \times e^{iqz}e^{\rho(q\cos\chi + ik\chi)}. \tag{4.1}$$

The second equality follows from Bessel's integral (Ref. [14], Sec. 2.21). We shall first assume that the wave-number weight function $w(k,q)$ is real, as it is for G_K. Then,

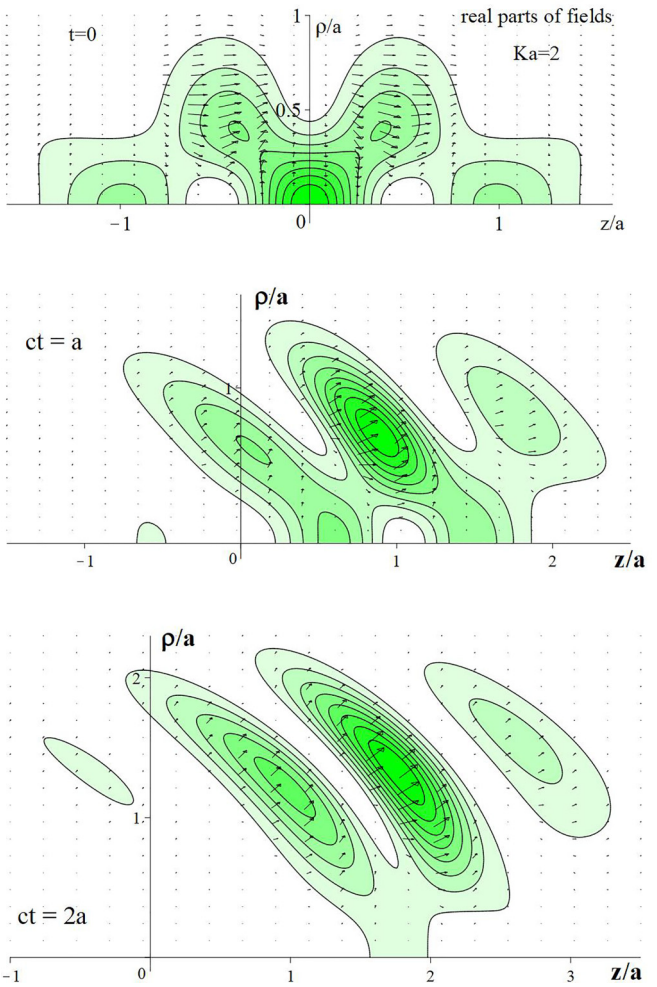

FIG. 1. Energy density (contours) and momentum density (arrows) of TE or TM pulses formed from *real part* of G_K, with $Ka = 2$ and at times $ct = 0,\ a,$ and $2a$. Propagation is from left to right. Three-dimensional picture is obtained by rotation about propagation axis (z axis).

the real part of ψ is

$$\psi_r = \frac{1}{2\pi}\int_{-\pi}^{\pi}d\chi\int_0^\infty dk\int_0^k dq w(k,q)e^{\rho q\cos\chi} \times \cos\{qz - kct + k\rho\sin\chi\}. \tag{4.2}$$

From (3.8) the z component of the momentum density is proportional to $-(\partial_\rho\partial_{ct}\psi_r)(\partial_\rho\partial_z\psi_r)$. The derivatives we need have integrands $w(k,q)$ times $e^{\rho q\cos\chi}\cos\{qz - kct + k\rho\sin\chi\}$. For $\partial_\rho\partial_z\psi_r$ and $\partial_\rho\partial_{ct}\psi_r$ the derivatives are, respectively,

$$-q\,e^{\rho q\cos\chi}\,[q\cos\chi\,\sin\{qz - kct + k\rho\sin\chi\} + k\sin\chi\,\cos\{qz - kct + k\rho\sin\chi\}], \tag{4.3}$$

$$k\,e^{\rho q\cos\chi}[q\cos\chi\,\sin\{qz - kct + k\rho\sin\chi\} + k\sin\chi\,\cos\{qz - kct + k\rho\sin\chi\}]. \tag{4.4}$$

The proof of the absence of backflow follows from the fact that the ratio of the integrands of $\partial_\rho\partial_z\psi_r$ and $\partial_\rho\partial_{ct}\psi_r$ is $-q/k$. In the integration over $k, q,$ and χ of the integrands

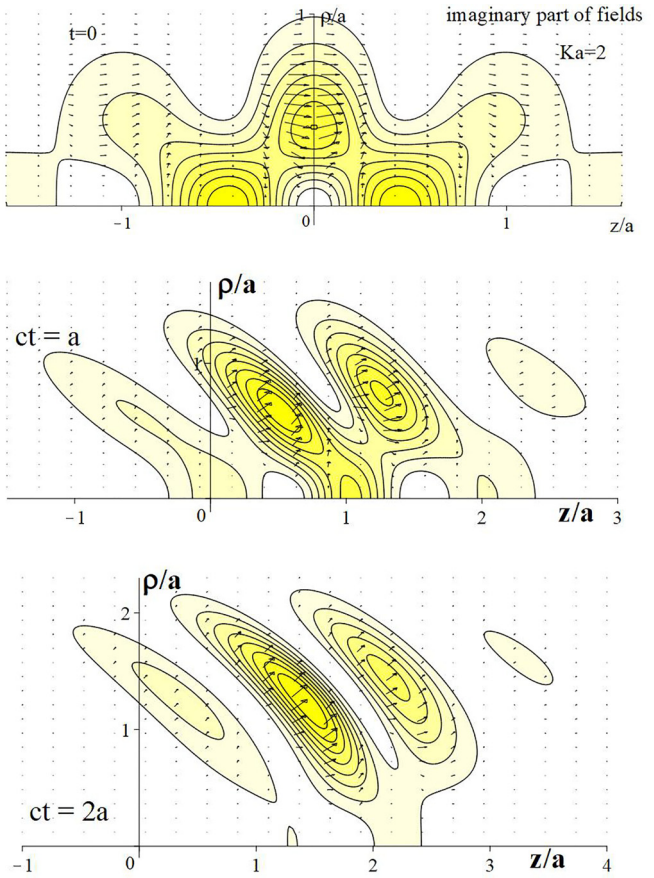

FIG. 2. Energy density (contours) and momentum density (arrows) of TE or TM pulses formed from *imaginary part* of G_K, with $Ka = 2$ and at times $ct = 0,\ a,$ and $2a$. Note that in contrast to real part in Fig. 1, energy and momentum densities are zero at space-time origin.

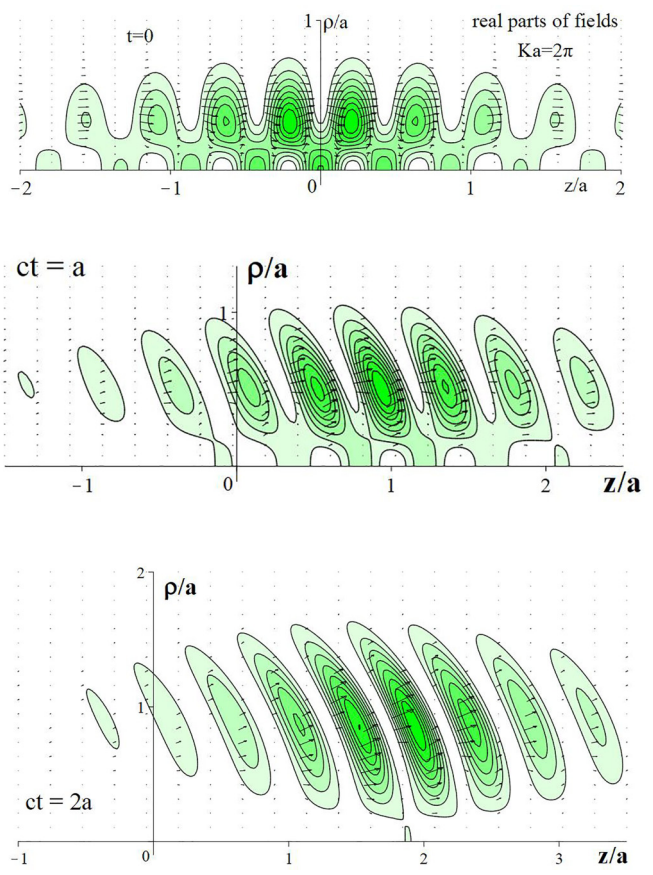

FIG. 3. Energy density (contours) and momentum density (arrows) of TE or TM pulses formed from real part of G_K, with $Ka = 2\pi$ and at times $ct = 0,\ a,$ and $2a$.

of $-\partial_\rho \partial_{ct}\psi_r$ and of $\partial_\rho \partial_z \psi_r$, the sign of these quantities will be the same at the same k, q, and χ. The same argument holds for the pulses based on the imaginary part of ψ. Thus p_z cannot be negative: backflow does not happen for TE and TM pulses based on G_K with real $w(k, q)$.

The integrands for general complex $w(k, q) = w_r(k, q) + iw_i(k, q)$ are also in the ratio $-q/k$. Any TE or TM pulse based on $m = 0$ wave functions of the form (4.1) will not have $p_z < 0$, anywhere.

It remains to consider general TE and TM pulses *with angular momentum*, based on solutions of the wave equation of the form (2.1), namely

$$\psi_m(\rho, \phi, z, t) = e^{im\phi} \int_0^\infty dk\, e^{-ikct} \int_0^k dq w(k, q) e^{iqz} J_m(\kappa\rho). \tag{4.5}$$

The z component of the momentum density is given by

$$4\pi c p_z = -m^2 \rho^{-2} (\partial_{ct}\psi_i)(\partial_z \psi_i) - (\partial_\rho \partial_{ct}\psi_r)(\partial_\rho \partial_z \psi_r). \tag{4.6}$$

In the first term on the right of (4.6) the integrands of $\partial_{ct}\psi_i$ and $\partial_z \psi_i$ are again in the ratio $-q/k$. Hence, the m^2 term is positive. In the second term we use the integral representation of $J_0(\kappa\rho)$, as in (4.1), and the fact that higher-order Bessel functions can be generated from $J_0(\kappa\rho)$ by repeated operation with $\partial_x + i\partial_y = e^{i\phi}(\partial_\rho + i\rho^{-1}\partial_\phi)$:

$$\{e^{i\phi}(\partial_\rho + i\rho^{-1}\partial_\phi)\}^m J_0(\kappa\rho) = (-\kappa)^m e^{im\phi} J_m(\kappa\rho). \tag{4.7}$$

The ratio of the integrands of $\partial_\rho \partial_z \psi_r$ and $\partial_\rho \partial_{ct}\psi_r$ is again $-q/k$, for any m and any complex weight function. TE or TM pulses based on wave functions of the form (4.5), with integer m and general $w(k, q)$, do not have backflow.

Backflow *does* exist near the focal plane of monochromatic beams, but it is weak and localized. See for example Figs. 3.2, 3.5, and 3.6 of Ref. [12], which show regions in which the cycle-averaged value of p_z for TE and TM beams is negative.

It is interesting to compare the focal regions of pulses and of monochromatic beams. There is a topological difference between the isophase surfaces in each: the *beam* surfaces of constant phase are concave towards the focal center, and are singular at circles on or near the focal plane. These singular points are at the zeros of the complex wave function (both ψ_r and ψ_i zero) at which the phase is not defined. Isophase surfaces corresponding to adjacent phases can meet on these circles, enabling the concave structure necessary for focal concentration (Sec. 1.6 of Ref. [12], and references therein). In contrast, the isophase surfaces of a scalar *pulse* have a topologically different structure. Figure 5 compares the isophase surfaces and moduli (at time zero) of a scalar pulse and of a scalar beam in their focal regions.

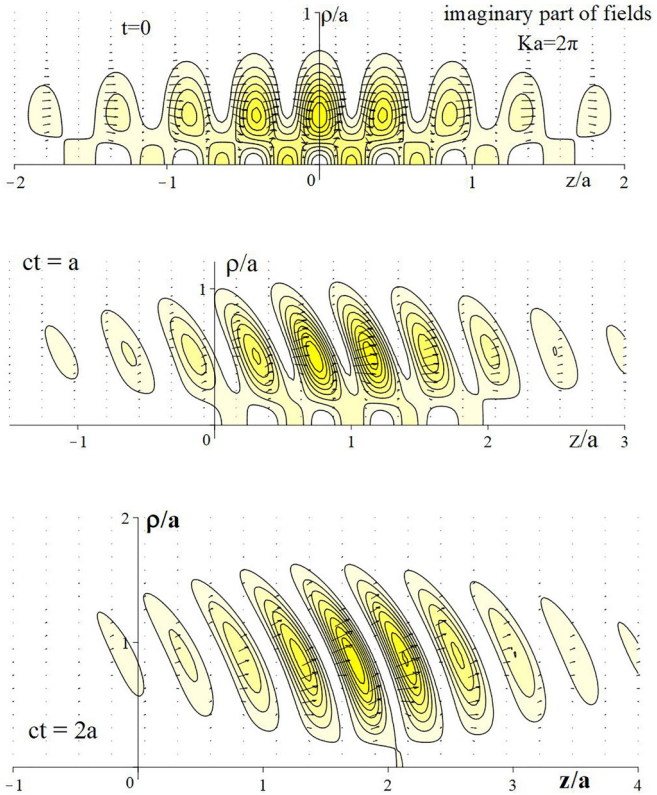

FIG. 4. Energy density (contours) and momentum density (arrows) of TE or TM pulses formed from imaginary part of G_K, with $Ka = 2\pi$ and at times $ct = 0,\ a,$ and $2a$.

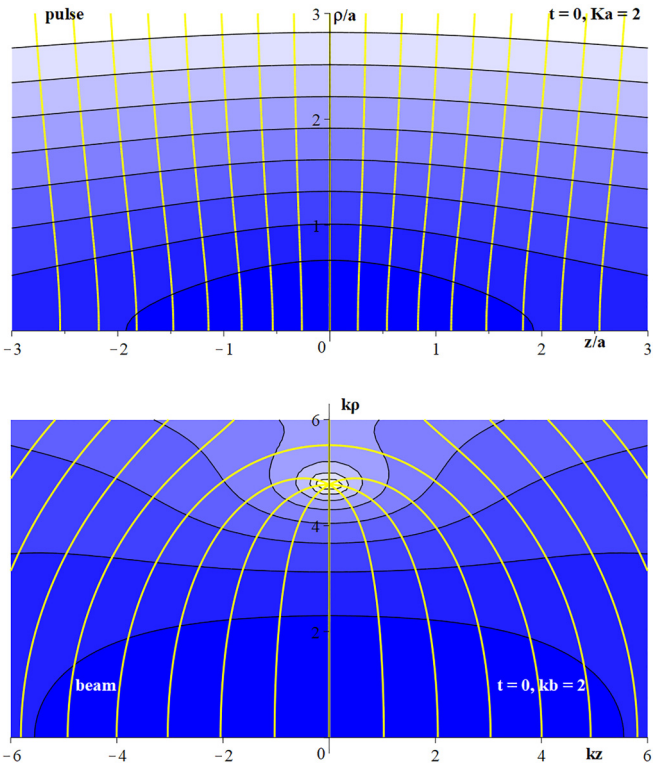

FIG. 5. Upper part: contours $|G_K|^2$, and isophase surfaces for scalar pulse G_K at time zero. Lower part: contours of $|\psi_b|^2$ and isophase surfaces for scalar beam of Eq. (4.9), again at $t = 0$. In both parts contours are of logarithms of moduli, and phase surfaces are at multiples of $\pi/4$. Propagation is from left to right.

For the pulse G_K, the modulus and phase at $t = 0$ are

$$|G_K(\rho, z, 0)| = \frac{a^2\, e^{K(a-\sqrt{a^2+\rho^2})}}{\sqrt{(a^2+\rho^2)(a^2+\rho^2+z^2)}},$$
$$P(\rho, z, 0) = Kz + \arctan\frac{z}{\sqrt{a^2+\rho^2}}. \tag{4.8}$$

The modulus has no zero except at infinity, and the phase varies smoothly, without singularity.

We shall compare the modulus and phase of the scalar pulse G_K with those of the scalar beam family ψ_b (Ref. [12], Sec. 2.6):

$$\psi_b(\rho, z) = \int_0^k dq\, q\, e^{q(b+iz)} J_0(\rho\sqrt{k^2-q^2}). \tag{4.9}$$

The time dependence e^{-ikct} is understood: the beams whose spatial dependence is defined in (4.9) are monochromatic, with angular frequency $\omega = kc$. The function $\psi_b(\rho, 0)$ is real, and has an infinity of zeros. The first zero, for $kb = 2$, lies on the circle $k\rho \approx 4.77, z = 0$. At the focal-plane zeros of ψ_b the surfaces of different phases can meet. Phases differing by multiples of 2π (such as $-\pi, \pi$ in the lower diagram of Fig. 5) can meet anywhere, since phase is defined as *mod* 2π.

V. EXTENT AND DIVERGENCE ANGLE OF TE AND TM PULSES BASED ON G_K

Figures 1 to 4 show that the TE and TM pulses based on G_K are annular. We wish to estimate the dependence on the length a and wave number K of the following:

(i) longitudinal and transverse extents,

(ii) number of annuli, and

(iii) angle of divergence from the axis of propagation.

It will help to use the spheroidal-like coordinates ξ, η, and ζ introduced in Appendix 2C of Ref. [3], in terms of which $\rho,\ z$, and ct are given by

$$\rho = a\sqrt{(\xi^2-1)(\eta^2+1)},\quad ct = a\xi\eta,\quad z = a\zeta. \tag{5.1}$$

The variable ranges are $1 \leqslant \xi < \infty,\ -\infty < \eta < \infty$, and $-\infty < \zeta < \infty$. The complex distance R becomes $R = a(\xi + i\eta)$, and the scalar pulse $G_K(\rho, z, t)$ of (1.3) and its modulus squared transform to

$$G_K(\xi, \eta, \zeta) = \frac{e^{Ka(1-\xi)} e^{iKa(\zeta-\eta)}}{(\xi+i\eta)[\xi+i(\eta-\zeta)]},$$
$$|G_K|^2 = \frac{e^{2Ka(1-\xi)}}{(\xi^2+\eta^2)[\xi^2+(\eta-\zeta)^2]}. \tag{5.2}$$

The modulus squared is a Lorentzian, with maximum on the axis ($\rho = 0,\ \xi = 1$) when $\zeta = \eta$, that is, at $z = ct$. It falls to half maximum when $\zeta = \eta \pm 1$. Thus defined, the *longitudinal extent* of the scalar pulse is $\Delta\zeta = 2$ or $\Delta z = 2a$. The dominant wave number is K, so we expect the number of oscillations within the wave packet to be of order Ka. The main factor determining the transverse extent of pulses derived from G_K is $e^{-2Ka\xi}$. The transverse extent is thus of order K^{-1}.

For the TE and TM pulses the momentum is zero on the axis, and the energy density has maxima on annuli. To apply the spheroidal-like coordinates, we need the derivatives. The z coordinate is just scaled, so $a\partial_z = \partial_\zeta$. The other derivatives are given by

$$a\partial_\rho = \frac{\sqrt{(\xi^2-1)(\eta^2+1)}}{\xi^2+\eta^2}(\xi\partial_\xi - \eta\partial_\eta),$$
$$a\partial_{ct} = \frac{-\eta(\xi^2-1)\partial_\xi + \xi(\eta^2+1)\partial_\eta}{\xi^2+\eta^2}. \tag{5.3}$$

The wave-equation operator $\nabla^2 - \partial_{ct}^2$ becomes a^{-2} times

$$\frac{(\xi^2-1)\partial_\xi^2 - (\eta^2+1)\partial_\eta^2 + 2\xi\partial_\xi - 2\eta\partial_\eta}{\xi^2+\eta^2} + \partial_\zeta^2. \tag{5.4}$$

The real and imaginary parts of G_K are

$$\psi_r = \frac{e^{Ka(1-\xi)}}{(\xi^2+\eta^2)[\xi^2+(\eta-\zeta)^2]}\{(\xi^2+\eta\zeta-\eta^2) \times \cos Ka(\eta-\zeta) - (2\eta-\zeta)\sin Ka(\eta-\zeta)\}, \tag{5.5}$$

$$\psi_i = \frac{e^{Ka(1-\xi)}}{(\xi^2+\eta^2)[\xi^2+(\eta-\zeta)^2]}\{(\xi^2+\eta\zeta-\eta^2) \times \sin Ka(\eta-\zeta) + (2\eta-\zeta)\cos Ka(\eta-\zeta)\}. \tag{5.6}$$

Both ψ_r and ψ_i annihilate $\nabla^2 - \partial_{ct}^2$ in the form (5.4).

The electric and magnetic fields of TE and TM pulses are given in terms of the derivatives of the wave function in Sec. III. On using (5.3) and the wave functions (5.5) or (5.6), we obtain expressions in the spheroidal-like coordinates ξ, η, and ζ. Of special interest are the energy densities u_r and u_i derived from the wave functions ψ_r and ψ_i of (5.5) and (5.6). These have the denominator

$$d = (\xi^2+\eta^2)^{10}[\xi^2+(\eta-\zeta)^2]^6. \tag{5.7}$$

There is thus a strong peaking around $\zeta = \eta$ (as there was in $|G_K|^2$ and in ψ_r and ψ_i). We therefore examine the energy density at $\zeta = \eta$. Far from the focal region (on the scale of the length a), and at positive times, the annular pulses diverge from the axis of propagation on a cone. We wish to estimate the polar angle θ at which they diverge. From the inverse relations to (5.1) (see equation (C7) in Chap. 2 of Ref. [3]), we find that

$$\xi = \frac{ct}{\sqrt{(ct)^2-\rho^2}} + O(a^2),$$
$$\eta = \frac{\sqrt{(ct)^2-\rho^2}}{a} + \frac{a\rho^2}{2[(ct)^2-\rho^2]^{3/2}} + O(a^3). \tag{5.8}$$

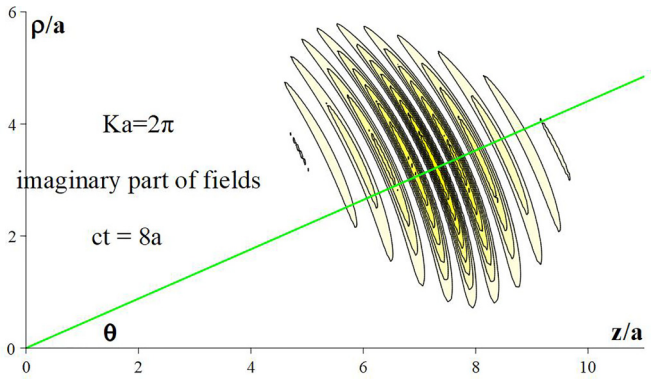

FIG. 6. Energy density contours at $ct = 8a$ for $Ka = 2\pi$ pulse based on ψ_i. Divergence angle $\theta \approx 23.8^\circ$ is found from (5.10).

On the cone of half-angle θ, and near the maximum energy density, we set $\rho = ct\sin\theta$ and $z = ct\cos\theta$. Then, with $C = \cos\theta$,

$$\xi \to C^{-1}, \quad \eta \to \frac{ct}{a}C + \frac{a}{2ct}(1-C^2)C^{-3}. \tag{5.9}$$

We examine the energy density based on ψ_i because this has a maximum on $r = \sqrt{\rho^2+z^2} = ct$, whereas that based on ψ_r has maxima on either side of $r = ct$, as seen in Figs. 1–4. With the substitutions (5.9), we find that the energy density is maximum on the angle determined by a quintic in $C = \cos\theta$:

$$2C^5 + 2KaC^4 + (Ka)^2C^3 + (Ka)^3C^2 - (Ka)^3 = 0. \tag{5.10}$$

For the Ka parameter values used in the figures, the divergence angles are $Ka = 2:\ \theta \approx 41.2^\circ$, and $Ka = 2\pi:\ \theta \approx 23.8^\circ$. When $Ka \gg 1$ the divergence angle θ tends to $(Ka)^{-1/2}$, in contradistinction to diffraction of a plane monochromatic wave of wave-number K through an aperture of size a, which has angular spread of order $(Ka)^{-1}$. Figure 6 shows the energy density of the ψ_i pulse at $ct = 8a$ when $Ka = 2\pi$.

VI. SUMMARY AND DISCUSSION

An exact oscillatory solution of the wave equation, characterized by a length a and a wave number K, is discussed and used to generate electromagnetic TE and TM pulses. The energy and momentum densities of these pulses are calculated, and the total energy and total momentum are found in two ways, in terms of a and K. The TE and TM pulses are annular, and converge onto or diverge from the axis of propagation, asymptotically on a cone, whose angle is determined.

These pulses, and all of the possible pulses that can be formed as a superposition of plane waves e^{iqz} multiplied by Bessel functions $J_m(\rho\sqrt{k^2-q^2})$, are shown to be *strictly forward propagating*, with momentum density $p_z \geqslant 0$ everywhere.

In this context, it is interesting to note that recent analyses of electromagnetic pulses [15,16] use the wave function (see Ref. [3], Sec. 2.3 for discussion of this function and its origins)

$$\psi(\rho,z,t) = \frac{ab}{\rho^2 + [a - i(z+ct)][z + i(z-ct)]}. \tag{6.1}$$

This wave function cannot be put in the form (2.1). Note the dependence on $z+ct$ as well as on $z-ct$. The modulus of (6.1) has maxima at $z=\pm ct$, and it was pointed out in Ref. [2] that the scalar pulse has *backward propagation*. For TE and TM pulses based on the real part ψ_r, the longitudinal component p_z of the momentum density, given in (3.8), has at $ct=-z$ and $|z|\gg a,b$, the leading term proportional to $a^2-2ab-3\rho^2$, which will be negative far from the axis, or at all ρ if $b>a/2$. The ratio of momentum densities at $ct=-z$ and $ct=z$ has negative leading term for large $|z|$:

$$\frac{p_z(ct=-z)}{p_z(ct=z)}=\frac{(a^2-2ab-3\rho^2)(a^2+2ab+3\rho^2}{a^8(4a^2b^2-b^4+12ab\rho^2+9\rho^4)}+O(z^{-2}). \tag{6.2}$$

For TE and TM pulses based on the imaginary part ψ_i, the situation is worse: the ratio of momentum densities at $ct=-z$ and $ct=z$ has negative leading term for large $|z|$:

$$\frac{p_z(ct=-z)}{p_z(ct=z)}=-\frac{b^6}{a^6}+O(z^{-2}). \tag{6.3}$$

In both cases the wave function (6.1) leads to unphysical backward propagation. The total momentum is however positive, provided $a>b$ (Ref. [3], Sec. 3.5 and references therein):

$$U=\frac{\pi}{16}\frac{a+b}{ab},\quad cP_z=\frac{\pi}{16}\frac{a-b}{ab}\quad(\psi_r \text{ or } \psi_i). \tag{6.4}$$

The above comments are in relation to the wave function (6.1), and in no way a criticism of the experimental results presented in [15] and [16].

A referee has drawn my attention to the paper by Smith and Strange [17], about chirality and the topology of field lines. Their fields are quite different: the electric and magnetic fields are the real and imaginary parts of the cross product of two gradients:

$$\boldsymbol{E}+i\boldsymbol{B}=E_0\nabla\alpha\times\nabla\beta, \tag{6.5}$$

$$\alpha=\frac{\rho^2+(z-ib)^2-(ct)^2}{\rho^2+z^2-(ct-ib)^2},\quad \beta=\frac{2b\rho e^{-i\phi}}{\rho^2+z^2-(ct-ib)^2}, \tag{6.6}$$

These fields are sufficiently localized for the pulse to have finite energy, momentum, and angular momentum. They are interesting topologically: the field lines are linked or knotted. The pulse is characterized by a single length b; it is not oscillatory. Of particular interest here is that the construction given above combines complex translation along z with the *same* complex translation along ct.

The complex translation $z\to z-ib$ along the propagation direction may be applied to generalize the pulses based on G_K discussed here, which have $ct\to ct-ia$ incorporated *ab initio*. The lengths a and b will in general be different. In contrast, with b replaced by a in the denominators of α and β, the fields defined above do not satisfy the Maxwell curl equations.

ACKNOWLEDGMENTS

This paper has benefited from the comments and a reference supplied by the referees.

[1] I. A. So, A. B. Plachenov, and A. P. Kiselev, Simple unidirectional finite-energy pulses, Phys. Rev. A **102**, 063529 (2020).
[2] J. Lekner, A family of localized and unidirectional pulses, Phys. Rev. A (to be published).
[3] J. Lekner, *Theory of Electromagnetic Pulses* (IOP Publishing, Bristol, 2018).
[4] J. Lekner, Electromagnetic pulses, localized and causal, Proc. R. Soc. A **474**, 20170655 (2018).
[5] A. Zangwill, *Modern Electrodynamics* (Cambridge University Press, Cambridge, 2013).
[6] M. von Laue, Zur Dynamik der Relativitätstheorie, Ann. Phys. **340**, 524 (1911).
[7] D. J. Griffiths, Resource Letter EM-1: Electromagnetic momentum, Am. J. Phys. **80**, 7 (2011).
[8] C. Møller, *The Theory of Relativity* (Oxford University Press, Oxford, UK, 1960).
[9] J. Lekner, Electromagnetic pulses which have a zero momentum frame, J. Opt. A: Pure Appl. Opt. **5**, L15 (2003).
[10] P. Andrejic, Lorentz transformation of electromagnetic pulses derived from Hertz potentials, arXiv:1706.09513.
[11] M. V. Fedorov and S. V. Vintskevich, Diverging light pulses in vacuum: Lorentz-invariant mass and mean propagation speed, Laser Phys. **27**, 036202 (2017).
[12] J. Lekner, *Theory of Electromagnetic Beams* (Springer, Berlin, 2022).
[13] P. Saari and I. Besieris, Backward energy flow in simple four-wave electromagnetic fields, Eur. J. Phys. **42**, 055301 (2021).
[14] G. N. Watson, *Theory of Bessel Functions*, 2nd ed. (Cambridge University Press, Cambridge, UK, 1966).
[15] Y. Shen, Y. Hou, N. Papasimakis, and N. I. Zheludev, Supertoroidal light pulses as electromagnetic skyrmions propagating in free space, Nat. Commun. **12**, 5891 (2021).
[16] A. Zdagkas, C. McDonnel, J. Deng, Y. Shen, G. Li, T. Ellenbogen, N. Papasimakis, and N. I. Zheludev, Observation of toroidal pulses of light, Nat. Photonics **16**, 523 (2022).
[17] G. Smith and P. Strange, Lipkin's conservation law in vacuum electromagnetic fields, J. Phys. A: Math. Gen. **51**, 435204 (2018).